GEOPHYSICAL RESEARCH LETTERS,VOL. 22, NO. 3, PAGES 299-302, FEBRUARY 1, 1995

Two-dimensional structure of slow shocks

N. Omidi,[1],M. Johnson, D. Krauss-Varban, and H. Karimabadi

Department of Electrical and Computer Engineering, University of California, San Diego, La Jolla

Abstract. The two-dimensional (2-D) structure of switch-off slow magnetosonic shocks is investigated using an electromagnetic hybrid (fluid electrons, kinetic ions) code. It is shown that the basic physical processes occurring at 1-D slow shocks are also operative in 2-D. Specifically, the interaction between the upstream ions and those streaming away from the shock results in the excitation of Alfvén/ion-cyclotron (AIC) waves. Depending on the plasma parameters, these waves may either stay in the upstream or convect back into the shock resulting in a non-steady shock behavior which prevents the formation of a trailing wave train. Despite this similarity, some slow shocks which are steady in 1-D are found to be non-steady in 2-D. Fourier analysis of the waves downstream of non-steady shocks identifies them as AIC, demonstrating that the waves remain on the same branch as they convect from upstream into the downstream region.

1. Introduction

Ever since the encounter of the ISEE-3 spacecraft with the slow shocks in the deep geomagnetic tail [e.g., *Feldman et al.*, 1984, 1985; *Smith et al.*, 1984; *Schwartz et al.*, 1987] there has been a renewed interest in the physics of slow magnetosonic shocks. One of the main reasons for this renewed interest lies in the marked contrast between the observed structures of these shocks and those predicted by the two-fluid theory [*Coroniti*, 1971] and early kinetic simulations [*Swift*, 1983; *Winske et al.*, 1985]. According to these studies, slow shocks are associated with a phase standing (dispersive) trailing wave train whose damping provides the necessary dissipation at the shock. The observations in the tail, however, did not provide any evidence for the presence of these waves. This posed a serious shortcoming in our understanding of slow shocks in that it was not clear what process provided the necessary dissipation at the shock. To address this problem a number of studies have been performed using hybrid (fluid electrons, kinetic ions) simulations [*Omidi and Winske*, 1989, 1992; *Lee et al.*, 1989; *Winske and Omidi*, 1990, 1992; *Vu et al.*, 1992]. These studies have found slow shock solutions with or without a trailing Alfvén wave train.

In the study by *Omidi and Winske* [1992] a number of different shock structures were found depending on the upstream plasma parameters. For example, one structure is associated with a dispersive Alfvén wave train in the downstream similar to that expected from the two-fluid theory. The wave train is generated by the cross-field currents at the shock via the process described by *Perez and Northrop* [1970]. In addition to the downstream waves, AIC waves are also found in the upstream region. These waves are excited by the interaction between the upstream ions and those backstreaming from the shock via the electromagnetic ion/ion-cyclotron (EMIIC) instability whose linear and nonlinear properties were investigated by *Winske and Omidi* [1990, 1992]. Another shock structure is associated with AIC waves in both the upstream and the downstream regions. In these shocks, the group velocity of the waves generated in the upstream is smaller than the flow speed. As a result, the waves get convected back into the downstream leading to a non-steady or a reforming shock behavior. It was shown that this non-steadiness prevents the formation of the phase standing Alfvén wave train.

In the studies by *Winske and Omidi* [1990, 1992], it was found that the maximum growth rates of the EMIIC instability occur at large angles with respect to the magnetic field (wave normal angle). This implied that for quasi-perpendicular (q-p) slow shocks, the maximum growth is expected to occur in the general direction of the shock normal. As a result, the use of 1-D simulations was a reasonable first approach. In general, however, the AIC waves are not expected to grow only along the shock normal and it is necessary to remove such a restriction from the simulations. To this end, we have recently used a 2-D hybrid code to investigate the structure of slow shocks the results of which are presented here. The plan of this paper is as follows. In the next section a brief description of the simulation model is given. The results of our study are presented in section 3. The last section gives a summary.

2. Numerical Model

A schematic of the simulation setup used in our study is shown in Figure 1. The simulation box is in the X-Y plane, has a dimension of 200×32 c/ω_p (ion inertial length) and is divided into 400×64 cells. The initial number of particles per cell is 40. Periodic boundary conditions are used in the $\bar{Y}$ direction. The upstream plasma is continuously injected from the left wall. Particles hitting the right-hand wall are specularly reflected into the box. This results in the formation of a slow shock which propagates to the left (see *Omidi and Winske*, 1992 for more details). Downstream of the shock the flow velocity along the X-direction is zero, but transverse acceleration across the shock causes a net flow in the $-Y$ direction. The upstream magnetic field lies in the X-Y plane and makes an angle of θ_{bn} (shock normal angle) with the X-axis. Downstream of the shock, the magnetic field has a smaller magnitude and in the switch-off shock limit it is entirely along the X-axis. Also shown in Figure 1 is an arrow anti-parallel

[1] Also at California Space Institute, University of California, San Diego, La Jolla.

Paper number 95GL00166
0094-8534/95/95GL-00166$03.00

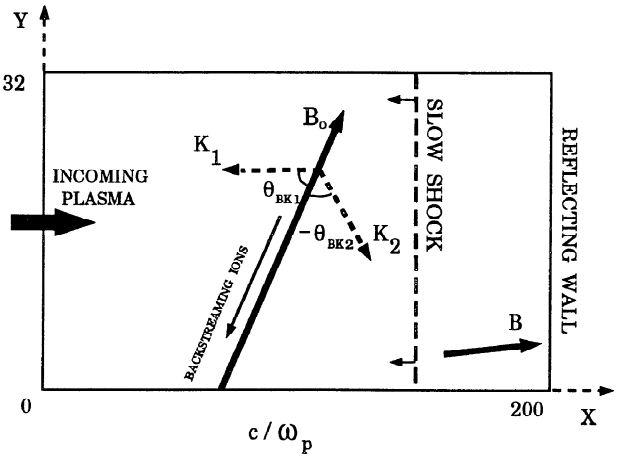

Figure 1. A schematic of the 2-D simulation box used in the study.

to the upstream magnetic field, representing the ions backstreaming (either reflected or escaping) from the shock. It is the interaction of these ions with the upstream plasma which excites AIC waves through the EMIIC instability.

In Figure 1 the two wave vectors $\vec{K}_1$ and $\vec{K}_2$ represent the waves that may grow due to EMIIC instability. Both the wavelength and the propagation direction of these waves may in general be different. Here, we have chosen a convention where $\vec{K}_2$ has a negative wave normal angle. Because the maximum growth rate

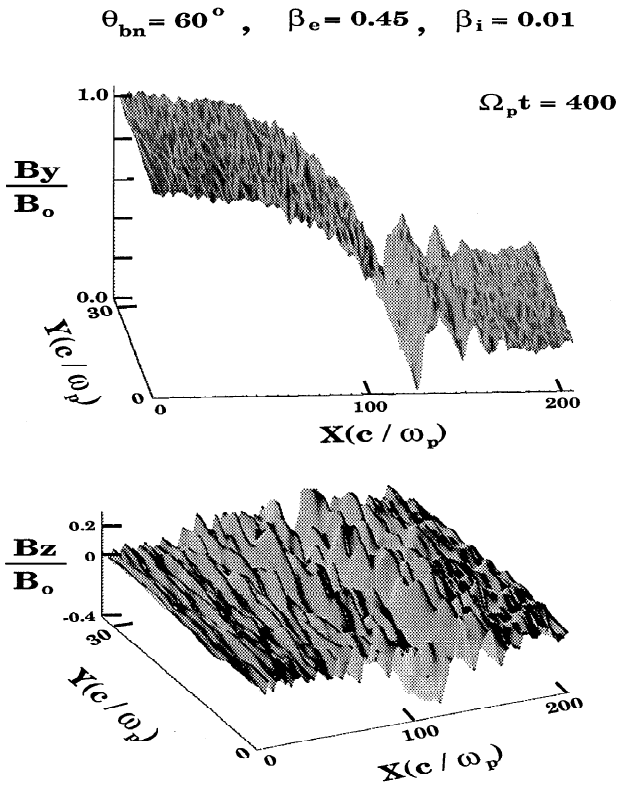

Figure 2. Plot of B_Y (compressional field component) and B_Z (transverse field component) as a function of X and Y for a steady slow shock.

of the EMIIC instability occurs at large angles, $\vec{K}_1$ is expected to be in the general direction of the X-axis for q-p shocks. But on the other hand, $\vec{K}_2$ has a large Y-component. Thus in 1-D simulations, one can at best capture $\vec{K}_1$, but the wave with $\vec{K}_2$ will be missed.

3. Results

The first case we consider is a switch-off slow shock with an intermediate Mach number of $M_I = 0.5$, $\theta_{bn} = 60°$, $\beta_e = 0.45$, and $\beta_i = 0.01$ where β is the ratio of kinetic to magnetic pressure. In *Omidi and Winske* [1992] it was found that this shock is steady with a trailing Alfvén wave train. Figure 2 shows the Y- and Z-components of the magnetic field as a function of X and Y at $\Omega_p t = 400$ for the same shock obtained from a 2-D hybrid simulation (Ω_p is the proton gyrofrequency). The shock is at $X \sim 125c/\omega_p$ and is associated with an Alfven wave train in the downstream region. In agreement with our expectation, the wave vector of these waves is along the shock normal direction (X-axis) which coincides with the downstream magnetic field direction. As a result, they are circularly polarized and have equal amplitudes in B_Y and B_Z.

In contrast, the waves seen in the upstream region are mostly evident in B_Z. These are obliquely propagating AIC waves excited by the EMIIC instability, which from linear theory, are expected to be linearly or elliptically polarized. Results of two-dimensional Fourier analysis (not shown here) indicate that these waves propagate at angles of $\theta_{BK} \sim \pm 30°$ with respect to the magnetic field which is considerably smaller than what was observed in *Omidi and Winske* [1992] (i.e. wave normal angle of 60°). Despite the difference in the propagation angle of the waves, however, the overall shock structure remains the same. This is because, as in the 1-D case, most of the AIC wave power in 2-D simulation stays in the upstream region and the shock remains steady.

We have also performed 2-D simulations of slow shocks which are unsteady in 1-D. The results have shown that the shock remains unsteady with an overall structure similar to its 1-D counterpart. In the remainder of this section we give an example of a slow shock whose 1- and 2-D structures are considerably different. The upstream parameters for this shock are $\theta_{bn} = 65°$ ($M_I = cos\ 65°$), $\beta_i = 0.01$, and $\beta_e = 0.1$. In the 1-D simulation, it was found that the shock is steady with an Alfvén wave train [*Omidi and Winske*, 1992]. Figure 3 shows the magnetic structure of the same shock obtained from a 2-D simulation. In contrast to its 1-D counterpart, this shock does not have a trailing wave train. However, the presence of wave activity in both the upstream and the downstream is quite evident. It can be seen from the top panel that the shock ramp is associated with large amplitude oscillations giving the shock a turbulent structure. The bottom panel in the figure shows wave activity both upstream and downstream of the shock. The latter waves have phase fronts which are more closely aligned in the Y-direction (more on this shortly). The absence of a dispersive wave train along with the presence of wave activity in the upstream and downstream suggest that the shock becomes unsteady in 2-D via the convection of the AIC waves from upstream into the downstream region. In general, this convection process can involve refraction and/or linear mode conversion across the shock. In the following we

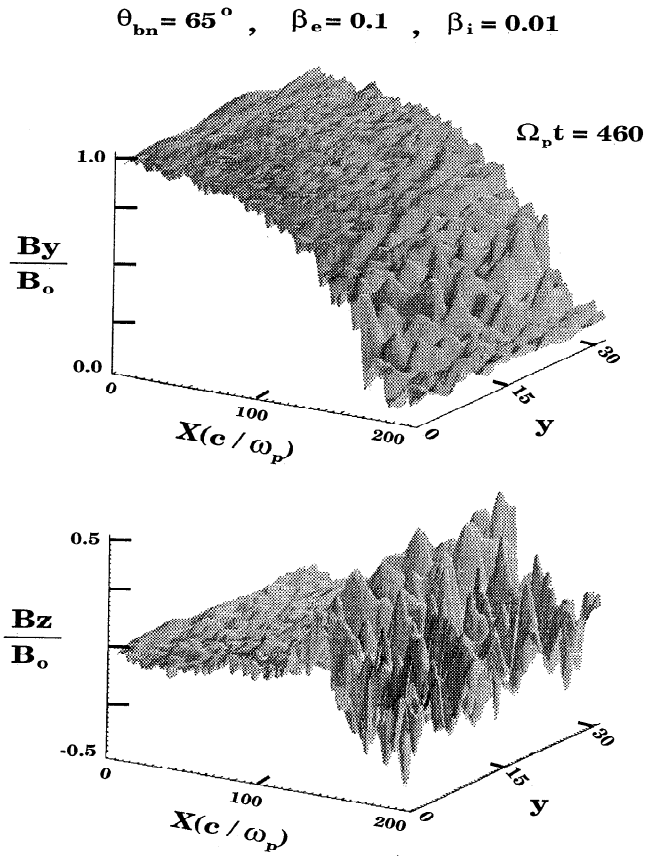

Figure 3. Same as in Figure 2 but for an unsteady slow shock.

consider the properties of the upstream and the downstream waves in more detail.

The top panel in Figure 4 shows the wave power in the three components of the magnetic field integrated over Y as a function of X at $\Omega_p t = 460$. The bottom panel shows B_Y averaged over Y as a function of X at the same time. As was shown by *Omidi and Winske* [1992], the presence of backstreaming ions forms a foot region where the magnetic field drops gradually. This foot is followed by a ramp which is associated with a much steeper field gradient. The top panel shows that wave activity begins within the foot region and it becomes stronger as one gets closer to the shock. The peak power occurs within and immediately downstream of the ramp. As can be seen, the power in B_Z is larger than the other two components of the field. This is consistent with obliquely propagating AIC waves which are elliptically polarized and their main magnetic field perturbation is out of the $\vec{K} - \vec{B}$ plane (i.e. B_Z).

To determine the wave propagation directions in the upstream and the downstream regions, we have conducted a two-dimensional Fourier analysis in space. The top two panels in Figure 5 show the wave power (in B_z) as a function of angle with respect to the X-axis (θ_{kx}) in the upstream ($160 \geq X \geq 130$) and the downstream ($200 \geq X \geq 175$) regions. In the upstream, the peak in power occurs at $\theta_{kx} \sim -50°$ corresponding to $\theta_{BK} \sim -65°$. Because of the decrease in B_y, however, the direction of the background magnetic field changes by a considerable amount within the chosen upstream region, and therefore θ_{BK} is not constant. The figure does, however, indicate that the waves with wave vector towards the shock have most of the power. This is in contrast to the 1-D simulation of the same shock and accounts for the big difference in their structure.

The results of Fourier analysis in the downstream region (top right panel in Figure 5) shows a peak at

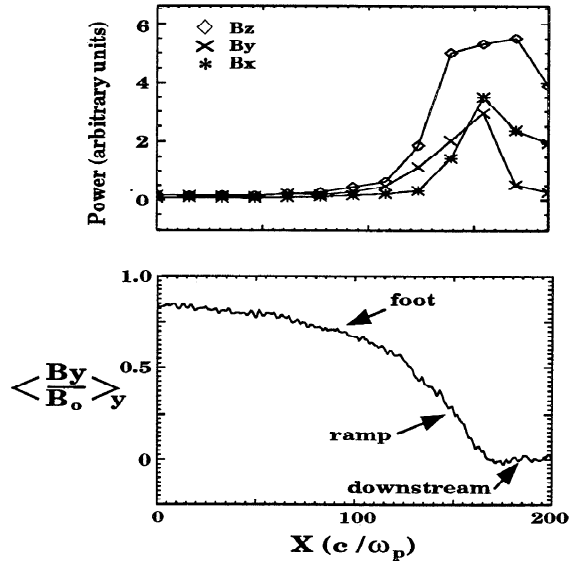

Figure 4. The top panel shows the wave power in B_X, B_Y, and B_Z averaged over Y as a function of X. The bottom panel shows the average shock profile (B_Y) as a function of X.

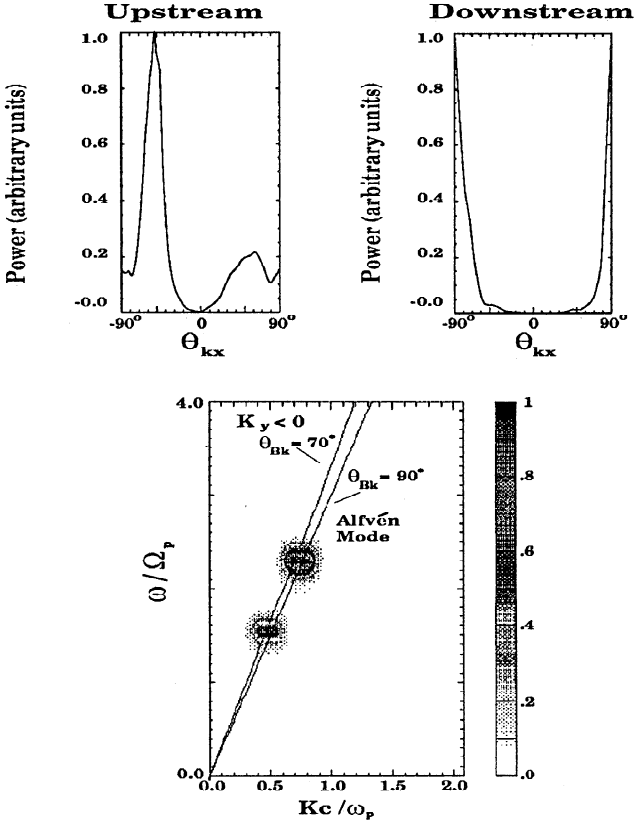

Figure 5. The top two panels show the power as a function of propagation angle in the upstream and the downstream regions. The bottom panel shows the power of the downstream waves as a function of ω and K.

$\theta_{kx} \sim \pm 90°$ which implies the waves are propagating along the Y-axis with the sign of K_Y to be determined by other means. A comparison between the top two panels in Figure 5 suggests that the waves are refracted as they convect from upstream to the downstream region. Although the upstream waves lie on the AIC branch, their mode of propagation may change as they convect into the downstream plasma which is characterized by a much higher beta $\beta_i = 3.65$, $\beta_e = 2.19$. To address this issue, we have conducted a 2-D Fourier analysis of the downstream waves in space (along the wave vector) and time which provides a power spectrum in the ω-K space. The bottom panel in Figure 5 shows the results of this analysis which was performed in the simulation frame of reference. Note that in this frame, the downstream plasma has a flow velocity $V_{flow} \sim -3\ V_{Ad}\ \vec{Y}$ (V_{Ad} is the Alfvén speed in the downstream region) which is caused by acceleration at the shock. The two solid lines shown in this panel are the dispersion relations of the AIC waves with $\theta_{Bk} = 70°$ and $90°$ Doppler shifted into the simulation frame. To perform the Doppler shift it was necessary to know the sign of K_Y. In Figure 5 the Doppler shifting was done assuming $K_Y < 0$ which is consistent with the upstream waves refracting as they convect into the downstream region. As can be seen, the wave power lies on the dispersion curve of the AIC mode demonstrating that the waves remain on the same branch as they cross the shock.

4. Summary and Discussion

The two-dimensional structure of switch-off slow shocks was investigated, and it was shown that the main physical processes occurring at 1-D shocks also occur at 2-D shocks. Specifically, both steady and reforming shock structures were found. In the former case the shock is associated with a dispersive Alfvén wave train in the downstream region and AIC waves generated by EMIIC instability in the upstream. Reforming or unsteady shocks occur when the AIC waves in the upstream get convected back into the shock. It was also shown that while some shocks which are steady in 1-D remain so in 2-D, others become unsteady in 2-D and as a consequence have a considerably different structure. Fourier analysis of the waves associated with unsteady shocks shows that maximum power occurs within and downstream of the ramp. Although the waves can be seen in all three components of the magnetic field, the amplitude of the oscillations outside of the $\vec{K} - \vec{B}$ plane is the largest. This is consistent with our expectations for AIC waves based on linear theory. Fourier analysis of the waves in the downstream shows that the dispersive properties of these waves match those of the AIC mode, demonstrating that they stay on the same branch as they convect from the upstream into the downstream region.

In this study we have found that the structure of some slow shocks can vary considerably from 1-D to 2-D simulations. On the other hand, it is very encouraging that the basic physical processes occurring at 1- and 2-D slow shocks are similar. This should allow for a detailed comparison between the observations and our current theoretical understanding of slow shocks. Although such studies remain to be carried out using the data from both ISEE-3 and the Geotail spacecrafts, a recent analysis of two slow shocks in the deep tail by *Coroniti et al.* [1994] is quite promising. According to this study, the two shocks are associated with transverse, polarized magnetic field oscillations with frequencies just below the ion cyclotron frequency. The power of these waves is largest within the shock ramp, similar to what has been shown in this paper. Other aspects of the observations, such as the wave amplitudes and the shock thickness are also in qualitative agreement with the simulation results. On the other hand, some of the basic properties of the observed waves, such as the mode and the direction of their propagation, is still unknown. It is hoped that future studies will shed further light on these issues.

Acknowledgments. This work was performed under the auspices of the California Space Institute, and was supported by NASA Space Physics Theory Program at UCSD (NAG 5-1492). The computations were performed on the CRAY Y-MP and CRAY C-90 at the San Diego Supercomputer Center which is supported by NSF.

References

Coroniti, F. V., Laminar wave train structure of collisionless magnetic slow shocks, *Nuclear Fusion*, *11*, 261, 1971.

Coroniti, F. V., et al., Magnetic and electric field waves in slow shocks of the distant geomagnetic tail: ISEE 3 observations, submitted to *J. Geophys. Res.*, 1994.

Feldman, W. C., et al., Evidence for slow mode shocks in the deep geomagnetic tail, *Geophys. Res. Lett.*, *11*, 599, 1984.

Feldman, W. C., et al., Slow-mode shocks: A semipermanent feature of the distant geomagnetic tail, *J. Geophys. Res.*, *90*, 233, 1985.

Lee, L. C., et al., Slow shock characteristics as a function of distance for the x-line in the magnetotail, *Geophys. Res. Lett.*, *16*, 903, 1989.

Omidi, N., and D. Winske, Structure of slow magnetosonic shocks in low beta plasmas, *Geophys. Res. Lett.*, *16*, 907, 1989.

Omidi, N., and D. Winske, Kinetic structure of slow shocks: Effects of the electromagnetic ion/ion cyclotron instability, *J. Geophys. Res.*, *97*, 14801, 1992.

Perez, J. K. and T. G. Northrop, Stationary waves produced by the Earth's bow shock, *J. Geophys. Res.*, *75*, 6011, 1970.

Petschek, H. E., Magnetic field annihilation, in AAS-NASA Symposium on the Physics of Solar Flares, edited by W. N. Hess, NASA Spec. Publ. SP-50, pp. 425, 1964.

Schwartz, S. J., et al., Electron dynamics and potential jump across slow mode shocks, *J. Geophys. Res.*, *92*, 3165, 1987.

Smith, E. J., et al., Slow mode shocks in the earth's magnetotail: ISEE-3, *Geophys. Res. Lett.*, *11*, 1054, 1984.

Swift, D. W., On the structure of the magnetic slow switch off shock, *J. Geophys. Res.*, *88*, 5685, 1983.

Vu, H. X., et al., Multiple slow switch-off shock solutions, *J. Geophys. Res.*, *97*, 13839, 1992.

Winske, D., et al., The structure and evolution of slow mode shocks, *Geophys. Res. Lett.*, *12*, 295, 1985.

Winske, D. and N. Omidi, Electromagnetic ion/ion cyclotron instability at slow shocks, *Geophys. Res. Lett.*, *17*, 2297, 1990.

Winske, D. and N. Omidi, Electromagnetic ion/ion cyclotron instability: Theory and simulations, *J. Geophys. Res.*, *97*, 14779, 1992.

N. Omidi, M. Johnson, H. Karimabadi, and D. Krauss-Varban, Department of Electrical and Computer Engineering, University of California, San Diego, 9500 Gilman Drive, La Jolla, California 92093-0407.

(received July 11, 1994; accepted September 15, 1994.)